A Markov Random Field Model for Bony Tissue Classification*

J.M. Pardo[1], D. Cabello[1] and J. Heras[2]

[1] Depto. Electrónica e Computación. Facultade de Física.
[2] Servicio de Ciruxía Ortopédica. Hospital Xeral de Galicia.
Universidade de Santiago de Compostela. SPAIN

Abstract 3D biomedical images constitute an indispensable source of information for the clinical diagnostic. In the case of bone structure images, a system that automatically interprets and presents a 3D shape reconstruction of the bone would be of great aid in areas such as bone remodeling, fracture prediction and prothesis design. In these tasks, external geometry needs to be precisely defined and lesions and pathologies identified. The object recognition task can rarely be carried out without knowledge on the domain. This knowledge may be introduced as a set of constraints over features and relationships between the regions obtained by means of a presegmentation. A formal scheme for the integration of this set of constraints and the solution of the interpretation problem is provided by the Markov Random Field (MRF) model. In this work we present a MRF model for identification of lesions and pathologies in the proximal tibia.

1 Introduction

Segmentation is a very important stage within the image analysis and interpretation processes. It must drive the recognition and finding of position of objects that are of interest. After the segmentation, a usually incomplete set of regions is obtained. The object recognition task can rarely be carried out without specific knowledge on the domain. This knowledge may be introduced as a set of constraints over properties and relationships between the regions obtained by means of a presegmentation. A frequent way of addressing this problem consists in growing regions by means of rule based systems. A recent example in the medical domain is the work by Sonka et al. (1996) . These methods often present dependencies on the initialization process and difficulties for incorporating global requirements. A formal scheme for the integration of a set of constraints and the solution of the interpretation problem is provided by the Markov Random Field (MRF) model (Modestino and Zhang, 1992; Kim and Yang, 1996). It permits relating local and global properties, which provides potential advantages in the incorporation of knowledge and in optimization. Many problems in vision may be stated as labeling problems in which the solution is a set of labels assigned to pixels or other features of the image (Li, 1995) . The *labeling problem* is specified in terms of a set of *sites*, $\mathcal{S} = \{1, \ldots, m\}$, and a set of labels, $\mathcal{L} = \{1, \ldots, M\}$. When each site is assigned a single label, $f_i = f(i)$, it may be taken as a function whose domain is $\mathcal{S}$ and

* This work was supported by Xunta de Galicia under Grant XUGA20603B96

whose image is $\mathcal{L}$, $f : \mathcal{S} \rightarrow \mathcal{L}$. Labeling with contextual constraints is indispensable for the interpretation of images. In terms of probabilities, contextual constraints may be locally expressed as a function of the conditional probabilities $P(f_i|\{f_{i'}\})$, where $\{f_{i'}\}$ denotes the set of labels in sites $i \neq i'$, or, globally as the joint probability $P(f)$. As the local information is more directly observed, the global inference is usually carried out based on local properties. The theory of MRFs provides a mathematical foundation for solving the problem of performing global inferences using local information.

In this work we interpret tibia CT images as a part of a system for the reconstruction of the 3D geometry of the bone for surgical planning of prosthesis implants (Pardo et al., 1995) . An objective of the system is the identification of lesions and pathologies present in the proximal tibia. In order to do this we will have to differentiate between cortical and trabecular bone and lesion. The latter is characterized by low density, high homogeneity and strong contrast with its neighbors. However, the low density within the trabecular bone as well as the low signal to noise ratio typical of medical images will result in the problem not being, in general, easy to solve. The work is structured into the following sections: In section 2 we introduce the theory of MRFs; in section 3 we describe the problem we address as well as the labeling through MRFs of each slice and the 3D interpretation of the labels. Finally, in section 4 we display the results.

2 MRF and Gibbs distributions

MRF theory is a branch of probability theory for the analysis of contextual dependencies of physical problems. It is used in labeling problems in order to establish probabilistic distributions of interacting labels. The sites in $\mathcal{S}$ are related to each other through a neighborhood system, that is defined as $\mathcal{N} = \{\mathcal{N}_i | \forall i \in \mathcal{S}\}$, where $\mathcal{N}_i$ is the set of neighbors of i. The neighborhood relationship presents the following properties: (1) a site is not a neighbor of itself: $i \notin \mathcal{N}_i$; and (2) the neighborhood relationship is mutual: $i \in \mathcal{N}_{i'} \iff i' \in \mathcal{N}_i$. For a set $\mathcal{S}$, the neighboring set of i is defined as the set of sites inside a radius r, $\mathcal{N}_i = \{i' \in \mathcal{S} \mid [dist(\text{feature}_{i'}, \text{feature}_i)]^2 \leq r, i' \neq i\}$, where $dist(\cdot,\cdot)$ must be adequately defined. The pair $(\mathcal{S},\mathcal{N})$ constitutes a graph $\mathcal{G}$, where $\mathcal{S}$ contains the nodes and $\mathcal{N}$ determines the arcs. An order n *clique* c is defined for $(\mathcal{S},\mathcal{N})$ as a subset of $\mathcal{S}$, consisting in collections of n neighboring sites:

$$\mathcal{C}_n = \{\{i^1, i^2, \ldots, i^n\} \mid i^1, i^2, \ldots, i^n \in \mathcal{S} \text{ are neighbors of one another}\}$$

Let $\mathcal{F} = F_1, \ldots, F_m$ be a family of random variables defined in the set $\mathcal{S}$, in which each variable F_i takes a value f_i in $\mathcal{L}$. The family $\mathcal{F}$ is called a random field. For a discrete set $\mathcal{L}$, the probability of random variable F_i taking the value f_i is denoted as $P(f_i)$, and the joint probability of $F_1 = f_1, \ldots, F_m = f_m$, is denoted as $P(f)$. $\mathcal{F}$ is a **MRF** over $\mathcal{S}$ with respect to $\mathcal{N}$ if and only if the following conditions are met: **positivity** $(P(f) > 0, \forall f \in \mathcal{F})$ and **Markovianity** $(P(f_i|f_{\mathcal{S}-\{i\}}) = P(f_i|f_{\mathcal{N}_i}))$. The equivalence between MRF and Gibbs distribution, proven by Hammersley and Clifford in 1971, provides a manageable mathematical way of specifying the joint probability of a MRF. A set of variables $\mathcal{F}$ is called a Gibbs Random Field (**GRF**) in $\mathcal{S}$ with respect to $\mathcal{N}$ if and only if it obeys a Gibbs distribution: $P(f) = Z^{-1} \times e^{-\frac{1}{T}U(f)}$, where $Z = \sum_{f \in \mathcal{F}} e^{-\frac{1}{T}U(f)}$ is called *partition function*, T *temperature*, $U(f)$ is the *energy function* defined as the sum of the clique potentials $V_c(f)$, which only depend on the

local configuration of the clique c, and $\mathcal{C}$ is the set of cliques under consideration. The joint probability $P(\mathcal{F} = f)$ may be specified by specifying the potential functions of the clique, which are defined as a function of the desired behavior. This way, the a priori knowledge is encoded. The most adequate estimation of the energy function when the a priori and likelihood distributions are known is to maximize a Bayes criterium. Out of these criteria, the most popular one in computational vision is *maximum a posteriori probability* (**MAP**) (Geman and Geman, 1984) . In the MAP scheme, the optimum solution is given by: $f^* = arg\max_{f\in\mathcal{F}} P(f|d) = arg\max_{f\in\mathcal{F}} p(d|f)P(f)$, where $P(f|d)$ is the a posteriori conditional probability of obtaining configuration f given observation d, $p(d|f)$ is the likelihood function of f for d fixed, and $P(f)$ is the a priori probability of the labeling f. In the MAP-MRF labeling this results in

$$f^* = arg\min_f U(f|d) = arg\min_f \{U(d|f) + U(f)\}.$$

3 CT image interpretation

In this work we present a system for the identification of lesions in the proximal tibia. We start by delimiting the external contour of the cortical bone through deformable contours (Pardo et al., 1997). Then, a low level oversegmentation (Cabello et al., 1993) of the bones is carried out. The information corresponding to this oversegmentation is organized into a region adjacency graph (**RAG**) in which the individual densitometric and morphometric properties of each region are stored and the neighborhood relationships are established through weighted arcs (magnitude of the shared surface). Then the identification of possible lesions in the bone starts. This process is divided into two parts: (1) identification of possible lesion zones in each slice of the 3D sequence for which we define a MRF and formulate the solution as a problem of MAP estimation; (2) 3D analysis of the lesion candidates based on their 3D continuity, size ratios, etc.

3.1 MRF model for labeling 2D regions

Let us have a set $\mathcal{R}$ of non homogeneous sites (RAG nodes), each one of them with an associated set of properties linked to others through contextual relationships. Let $\mathcal{L}$ be the set of labels. Assume that the structure of the scene is represented by $\mathcal{G} = (\mathcal{R}, d)$, and that of the model by $\mathcal{G}' = (\mathcal{L}, D)$; where d and D refer to properties and relationships between the respective features. The features extracted from the image, $d = \{d_1, d_2\}$, are both unary properties d_1 of regions (area, perimeter, mean density, variance, etc.) and binary relationships d_2 (adjacency, hole of, etc.). The model includes a set of properties D. We consider that observation d, under configuration f, is a version of the features D of the model contaminated with white Gaussian noise n: $d_1(i) = D_1(f_i) + n(i)$, $d_2(i, i') = D_2(f_i, f_{i'}) + n(i, i')$, therefore $d_1(i)$ and $d_2(i, i')$ are Gaussian mean distributions $D_1(f_i)$ y $D_2(f_i, f_{i'})$. With clique potentials of up to two sites the energy takes the form $U(f|d) = U(f) + U(d|f) = \sum_{i\in\mathcal{R}} V_1(f_i) + \sum_{i\in\mathcal{R}} \sum_{i'\in\mathcal{N}_i} V_2(f_i, f_{i'}) + \sum_{i\in\mathcal{R}} V_1(d_1|f_i) + \sum_{i\in\mathcal{R}} \sum_{i'\in\mathcal{R}-\{i\}} V_2(d_2(i, i')|f_i, f_{i'})$ This expression with cliques of up to the second order is the simplest form that is able to contain contextual information. The first two terms refer to the a priori joint probability and the last two consider the likelihood function of f given a fixed d. The interpretation of the image is formulated as a MAP estimation problem.

Clique potentials For the case of detecting lesions in tibia images, the set of labels would be of the form $\mathcal{L} = \{\text{lesion}, \text{bone}\} = \{-1, 1\}$. The neighborhood relationship will be weighed by the shared edge. The lesion areas within the bone are characterized by their low density, homogeneity and compact shape, as opposed to the characteristics of high mean density (cortical bone) or high variance (trabecular bone). We have chosen the following clique potentials for the MRF model that allow us to identify the lesion areas. For the a priori energy we have:

$$V_1(f_i) = \alpha_i \tag{1}$$

$$V_2(f_i, f_{i'}) = \begin{cases} \beta(f_i - 1)f_{i'} + \beta_{ii'} \text{ if} f_i = -1 \& f_{i'} = 1 \& (N_{i,i'} = P_{i'} | N(i, i') = P_i) \\ \beta(f_i - 1)f_{i'} \qquad \text{other case} \end{cases} \tag{2}$$

where $N_{i,i'}$ denotes the shared contour or degree of neighborhood between the two regions; P_i represents the perimeter of region i. The condition $(N_{i,i'} = P_{i'} \mid N_{i,i'} = P_i)$ means that one of the regions is a hole in the other. With these clique potentials we define the a priori energy by just summing over all the cliques in $\mathcal{R}$. The potential for first order cliques penalizes the label with a highest relative value of α. The potential for second order cliques penalizes regions that are labeled as lesions that have holes with any label and regions labeled as bone that are holes of regions labeled as lesions. The penalty varies depending on the label of the hole and the region that contains it. Obviously, a region that is finally labeled as a lesion cannot contain bone holes, but it can contain lesion holes, as in the end they will unite as a single lesion region. Finally, the labeling of continuous lesions is penalized. For the conditional energy we have the following clique functions:

$$V_1(d_1(i)|f_i) = \begin{cases} \min\{1.0, \frac{[\rho_i + \sigma_i]^2}{2\sigma^2_{\rho\sigma}}\} & \text{if } f_i = -1 \\ \min\{1.0, \frac{[\min\{0, (\rho_i + \sigma_i) - \rho_b\}]^2}{2\sigma^2_{\rho\sigma}}\} & \text{if } f_i = 1 \end{cases} \tag{3}$$

$$V_2(d_2(i, i')|f_i, f_{i'}) = \begin{cases} \gamma(1 - 2f_i)\frac{N_{i,i'}[(\rho_i + \sigma_i) - (\rho_{i'} - \sigma_i)]}{P_i(\rho_i + \sigma_i)} & \text{if } f_i \neq f_{i'} \\ 0 & \text{other case} \end{cases} \tag{4}$$

defining the conditional p.d.f. of the observed data (features and relationships). Depending on the label, each region is assigned a different first order clique potential. For the case of lesions, high densities and variances are penalized. For the case of bones, the situation is more complex as bone tissues may present either high density and low variance (cortical bone) or high variance and medium-low density. To consider these two cases, we define the clique potential as the square of the distance from the mean value (ρ_i) plus variance (σ_i) and null density in the case of region labeled as lesion and a high value (ρ_b) for the case of bone label. The two measures are bounded between 0 and 1 adopting the form of the Blake-Zisserman potential. The second order clique potential refers to the contrast between regions. It terms a region as a lesion when it is less dense than its bone neighbors and penalizes it otherwise. The same happens with the bone labels. The term is weighed by the length of the contour shared by the two regions.

The p.d.f. is still not completely characterized by just providing the form of the clique potentials. It is necessary to also determine the value of the parameters present

in the expression of these potentials. The mean values and variances may be easily determined from the image. In order to obtain these values for the expressions of the first order clique potentials for the conditional probability distribution function of the observed data we have evaluated the mean density ($\overline{\rho}$) and the mean variance ($\overline{\sigma}$) in the muscular tissue regions adjacent to the cortical bone. We choose $\rho_b = 3(\overline{\rho} + \overline{\sigma})$ and $\sigma^2_{\rho\sigma} = 4.5(\overline{\rho} + \overline{\sigma})^2$. As what is important are not the absolute values of the parameters but their relative value, we consider the former as fixed and we will just have to set parameters $\alpha_i, \beta, \beta_{ii'}, \gamma$. As the learning of the parameters is difficult to carry out, we have decided on a manual parameter fit that permits recognizing an excessive number of possible lesion regions. Later, in the application of the second labeling stage, we will discriminate between true and false lesions by means of the application of rules regarding 3D continuity. We start from a random labeling of the regions provided by the presegmentation to which we apply the *simulated annealing* (Kirkpatrick et al., 1983) optimization method, as it would determine the global minimum with a reasonable cost. As a result of this labeling we would have a region map with lesion and bone labels. There will be adjacent regions that are labeled as lesion and thus an immediate step consists in joining these regions into a single one. The labeling obtained up to this point would not be in general correct because many small regions corresponding to holes in the trabecular region may have been labeled as lesions. In addition, certain regions that are not small but which present a low density will also be labeled as a lesion. In an initial filtering operation we eliminate the very small regions and those of very irregular shape. This consists in a label change, that in a later processing stage may be recovered if the 3D information demands it. It is a reversible process.

3.2 3D analysis

Once the 2D images have been analyzed, a set of regions with lesion label and another with a bone label are obtained. The low signal to noise ratio of the images, as well as a low density trabecular structure may often lead to erroneous labeling. The labeling may be improved if now we analyze the resulting configurations by means of a rule based system in which constraints on 3D continuity, bifurcations, area relationships between 2D sections of the same 3D lesion, connection of the 3D lesion with the outside, etc., are considered. Initially, we apply rules regarding 3D continuity of the 2D lesion regions:

IF: [1] $f_i = -1$ [2] $A_i^k < A_{TH}$
THEN: [1] $f_i = 0$
IF: [1] $f_i^k = -1$ [2] $\exists\ n > 2$ $j_n^{(k+\nu)}$ so that $N_{i^k, j_n^{(k+\nu)}} > 0$
THEN: [1] $f_i = 0$ [2] $f_{j_n}^{(k+\nu)} = 0$, $\forall j_n \in$ slice $k+\nu$
IF: [1] $f_i^k = -1$ [2] $\exists$ 2 $j_n^{(k+\nu)}$ so that $N_{i^k, j_n^{(k+\nu)}} > 0$ with $n = \{1,2\}$
[3] $\nexists\ p^{(k+\nu)}$ so that $N_{p^{(k+\nu)}, j_n^{(k+\nu)}} > 0$ with $n = \{1,2\}$
THEN: [1] $f_i = 0$ [2] $f_{j_n}^{(k+\nu)} = 0$, $n = \{1,2\}$
IF: [1] $f_i^k = -1$ [2] $\exists$ 2 $j_n^{(k+\nu)}$ so that $N_{i^k, j_n^{(k+\nu)}} > 0$ with $n = \{1,2\}$
[3] $\exists\ p^{(k+\nu)}$ so taht $N_{p^{(k+\nu)}, j_n^{(k+\nu)}} > 0$ with $n = \{1,2\}$
[4] $A_{p^{(k+\nu)}} + A_{j_1^{(k+\nu)}} + A_{j_2^{(k+\nu)}} < \alpha A_{i^{(k)}}$
THEN: [1] Merging: $j_1^{(k+\nu)} = j_1^{(k+\nu)} \cup j_2^{(k+\nu)} \cup p^{(k+\nu)}$
IF: [1] $f_i^k = 0$ [2] $f_j^{(k+\nu)} \neq -1$, $\forall j$ so that $N_{i^k, j^{(k+\nu)}} > 0$
THEN: [1] $f_i^k = 1$

where superindex k refers to the slice number, $k+\nu$, with $\nu \in \{-1,1\}$ referring to two adjacent slices and $N_{i^k,j^{(k+\nu)}}$ represents the overlap between region i of slice k and region j of one of the neighboring slices. These rules are applied in order so that initially all the slices are explored seeking the continuity of the lesion. Independently from their 3D continuity, a region with a possible lesion label is labeled as null if its area A_i^k is less than a threshold A_{TH}. This is done in order to discard narrow volumes labeled as lesions but that correspond to holes in the trabecular structure. If a lesion in a slice has a single continuity in its neighbors it preserves the label. If it only presents continuity in one of the slices or at least in one of them it presents continuity in more than two regions the region of the current slice and the neighboring slices with multiple continuity are assigned a null label. If it presents continuity in two slices but it is equal to two in one of them and there is no contact region such that the union of the three regions of the neighboring slice has an area of less than α times the area of the region in the current slice, all of them are assigned a null label. If the contact region exists, the three regions are joined into a single one. In the second pass those regions that do not have any neighbor with the label of bone are labeled as bone.

First a region growing is performed in 3D. A list of nodes is created, each one representing a possible 3D lesion (L_i) with the following information:

- Number of extreme slices affected by the lesion L: z^L_{min}, z^L_{max}.
- Number of 2D regions that make up the region: num_regs. This number is different from $z^L_{max} - z^L_{min} + 1$ when the 3D region of possible lesion presents bifurcations.
- Center of masses of the lesion: $\bar{r} = (\bar{x}^L, \bar{y}^L, \bar{z}^L)$.
- Mean area of the 2D regions that make up the lesion : $\bar{A}^L$.
- List of pointers to the regions of the RAG that are a part of the lesion: $R^L_1 \ldots, R^L_m$.

The following processing would affect the whole lesion. Initially we seek lesions that are aligned with the z axis and with their extremes very close together. This case would be due to a bad labeling of intermediate regions that could have divided the lesion. The 3D regions that do not encompass a minimum number of slices and are not connected to the background will be taken as low density bones and the label of bone will be assigned to them. The remaining ones will be classified as lesion and will be smoothed incorporating 2D neighbors that increase the regularity of the shape. This incorporation will occur for regions the presegmentator detects as transition between bone and lesion when they are really lesions. This process is carried out iteratively over the whole volume until there are no more incorporations. Finally, an evaluation of the smoothness of the region is performed, assigning it a bone label in the case it does not surpass a minimum value for the smoothness. Out of the remaining lesions we have to consider the lesion bifurcation cases. Here we will preserve the longest path, discarding the remaining bifurcations, as it is the most probable one having overcome all the previous constraints. In general the rest of the bifurcations are usually much shorter. This processing is summarized in the set of rules we now indicate:

IF : [1] $dist_1(L_i - L_j) = \min\{|z^{L_i}_{min} - z^{L_j}_{max}|, |z^{L_j}_{min} - z^{L_i}_{max}|\} \leq \epsilon_d$

[2] $dist_2(L_i - L_j) = ||\bar{r}^{L_i} - \bar{r}^{L_j}|| < \max\{\frac{\bar{A}^{L_i}}{\pi}, \frac{\bar{A}^{L_j}}{\pi}\}$

THEN : [1] $L_{ij} = \text{UNION}(L_i, L_j)$

IF : [1] $z^{L_i}_{max} - z^{L_i}_{min} < \epsilon_z$ [2] $\text{ADJACENCY}(R^{L_i}_k, \text{background}) = 0, \quad \forall k \in L_i$

THEN : [1] $f_{R^{L_i}_k} = 1, \quad \forall k \in L_i$

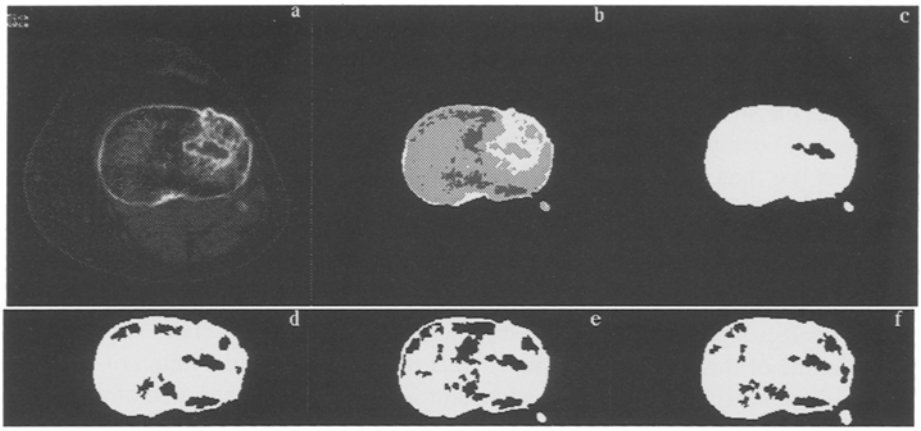

Figure1. (a) original image, (b) presegmentation, (c) final labeling, (d)-(f) intermediate labeling of contiguous slices.

$$\textbf{IF:}\quad [1]\ \epsilon_{A,1} \leq \frac{\text{AREA}(R_i^{k+\nu,L_i})}{\text{AREA}(R_j^{k,L_i})} < \epsilon_{A,2} \quad \nu \in \{-1,1\}$$

$$[2]\ ADJACENCY(R_j^{k,L_i}, R) > 0 \quad [3]\ \frac{\text{COMPACTNESS}(R_j^{k,L_i \cup R})}{\text{COMPACTNESS}(R_i^{k,L_i})} > \epsilon_c$$

$$\textbf{THEN:}[1]\ R_j^{k,L_i} = R_j^{k,L_i} \cup R$$

$$\textbf{IF:}\quad [1]\ \epsilon_{A,1} \leq \frac{\text{AREA}(R_i^{k+\nu,L_i})}{\text{AREA}(R_j^{k,L_i})} < \epsilon_{A,2} \quad \nu \in \{-1,1\} \quad [2]\ ADJACENCY(R_j^{k,L_i}, R) > 0$$

$$[3]\ \text{OVERLAY}(R_i^{k+\nu,L_i}, R) > \epsilon_o \quad [4]\ \frac{\text{AREA}(R_j^{k,L_i \cup R})}{\text{AREA}(R_i^{k+\nu,L_i})} < \epsilon_{A,2}$$

$$\textbf{THEN:}[1]\ R_j^{k,L_i} = R_j^{k,L_i} \cup R$$

$$\textbf{IF:}\quad [1]\ \#ND = \{i |\ \epsilon_{A,3} \geq \frac{\text{AREA}(R_i^{k+1,L_i})}{\text{AREA}(R_j^{k,L_i})} < \epsilon_{A,4}\} > \epsilon_{nd}$$

$$\textbf{THEN:}[1]\ f_{R_j^{k,L_i}} = 1, \quad \forall j,k \in L_i$$

4 Results

To illustrate the behavior of the system we have processed a sequence of transverse CT scan proximal tibia slices obtained in vivo from a 62 year old patient who had suffered a fracture of the external tibia plateau one year before. After that, the patient developed a posttraumatic osteoarthritis due to bone loss at the tibial plateau. In order to evaluate the type of defect an automatic 3D reconstruction was done. The images were preprocessed slice by slice in order to obtain the external contours of the tibia and fibula by means of deformable contours and from them, oversegment the enclosed regions. From this presegmentation we constructed the RAG that constitutes the input to the lesion labeling system. In Fig. 1a we represent an intermediate slice in which a central defect with a solid cortical shell of bone all around appears. It may be observed how there are bone areas that apparently present a lower intensity than the lesion. Because of this, in the

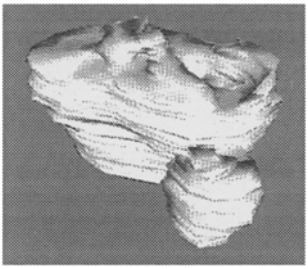

Figure2. 3D surface reconstruction of the tibia with a central defect.

labeling they appear with a label of lesion regions of the trabecula (Figure 1e). In the slice sequence, Figure 1(d-f), it can be observed how the true lesion region preserves a shape and size that is similar in all 3 slices, whereas this is not so in the other cases. With the 3D processing based on continuity of size and shape, minimum length and connection to the outside, we achieve the correct labeling Figure 1c. Finally, Fig. 2 shows 3D views of the proximal tibia which was extracted by the system. We can see that the patient presents a central defect with a solid cortical shell of bone all around.

References

1. M. Sonka, W. Park, and E. A. Hoffman. Rule-based detection of intrathoracic airway trees. *IEEE Transactions on Medical Imaging*, 15(3):314–326, June 1996.
2. J. W. Modestino and J. Zhang. A Markov random field model–based approach to image interpretation. *IEEE Trans. Patt. Anal. Machine. Intell.*, 14(6):606–615, 1992.
3. I. Y. Kim and H. S. Yang. An interpretation scheme for image segmentation and labeling based on Markov random field model. *IEEE Trans. Patt. Anal. Machine. Intell.*, 18(1):69–73, 1996.
4. S. Z. Li. *Markov Random Field Modeling in Computer Vision*. Springer–Verlag, Tokio, 1995.
5. J. M Pardo, D. Cabello, M. J. Carreira, M. G. Penedo, and J. Heras. Knowledge-based CT image analysis: automatic 3d shape reconstruction of bones. In *Proc. of the Second Asian Conference on Computer Vision*, volume I, pages 504–508, 1995.
6. S. Geman and D. Geman. Stochastic relaxation, Gibbs distribution, and Bayesian restoration of images. *IEEE Trans. Patt. Anal. Machine. Intell.*, 6(6):721–741, 1984.
7. J. M Pardo, D. Cabello, M.J. Carreira, and J. Heras. Integrating region and edge information in CT image segmentation. In A. Sanfeliu, J.J. Villanueva, and J. Vitria, editors, *Patern Recognition and Image Analysis*, volume 1, pages 7–12. 1997.
8. D. Cabello, M. G. Penedo, S. Barro, J. M. Pardo, and J. Heras. CT image segmentation by self–organazing learning. In J. Mira, J. Cabestany, and A. Prieto, editors, *New trends in neural computation*, volume 686, pages 651–656. Spring-Verlag, 1993.
9. S. Kirkpatrick, C. D. Gelatt, and M. P. Vecchi. Optimization by simulated annealing. *Science*, 220:671–680, 1983.